Genetic dissection of an ancient divergence in yeast thermotolerance

Carly V. Weiss[1], Jeremy I. Roop[1,2]*, Rylee K. Hackley[1,3,4], Julie Chuong[3], Igor V. Grigoriev[1,5], Adam P. Arkin[6], Jeffrey M. Skerker[6], Rachel B. Brem[1,3]*

[1]Department of Plant and Microbial Biology, UC Berkeley, Berkeley, CA.

[2]Current address: Fred Hutchinson Cancer Research Center, Seattle, WA.

[3]Buck Institute for Research on Aging, Novato, CA.

[4]Current address: Duke University Program in Genetics & Genomics, Duke University, Durham, NC.

[5]US Department of Energy Joint Genome Institute, Walnut Creek, CA.

[6]Department of Bioengineering, UC Berkeley, Berkeley, CA and Lawrence Berkeley National Laboratory, Berkeley, CA.

*Correspondence to: jeremyianroop@gmail.com, rbrem@buckinstitute.org.

Abstract

Some of the most unique and compelling survival strategies in the natural world are fixed in isolated species. To date, molecular insight into these ancient adaptations has been limited, as classic experimental genetics has focused on interfertile individuals in populations. Here we use a new mapping approach, which screens mutants in a sterile interspecific hybrid, to identify eight housekeeping genes that underlie the growth advantage of *Saccharomyces cerevisiae* over its distant relative *S. paradoxus* at high temperature. Pro-thermotolerance alleles at these mapped loci were required for the adaptive trait in *S. cerevisiae* and sufficient for its partial reconstruction in *S. paradoxus*. The emerging picture is one in which *S. cerevisiae* improved the heat resistance of multiple components of the fundamental growth machinery in response to selective pressure. This study lays the groundwork for the mapping of genotype to phenotype in clades of sister species across Eukarya.

Geneticists since Mendel have sought to understand how and why wild individuals differ. Studies toward this end routinely test for a relationship between genotype and phenotype via linkage or association[1]. These familiar approaches, though powerful in many contexts, have an important drawback—they can only be applied to interfertile members of the same species. This rules out any case in which an innovation in form or function evolved long ago and is now fixed in a reproductively isolated population.

As organisms undergo selection over long timescales, their traits may be refined by processes quite different from those that happen early in adaptation[2,3]. We know little about these mechanisms in the wild, expressly because when the resulting lineages become reproductively incompatible, classic statistical-genetic methods cannot be used to analyze them[4]. To date, the field has advanced largely on the strength of candidate-based studies that implicate a single variant gene in an interspecific trait[5,6], with the complete genetic architecture often remaining unknown. Against the backdrop of a few specialized introgression[7-10] and molecular-evolution[11] techniques available in the field, dissection of complex trait differences between species has remained a key challenge.

Here we develop a new genetic mapping strategy, based on the reciprocal hemizygosity test[12,13], and use it to identify the determinants of a difference in high-temperature growth between isolated *Saccharomyces* yeast species. We validate the contributions of the mapped loci to the thermotolerance trait, and we investigate their evolutionary history.

Results

Species differences in thermotolerance

57

58 At high temperature, the yeast *Saccharomyces cerevisiae* grows qualitatively better than other
59 members of its clade[14-16], including its closest relative, *S. paradoxus*, from which it diverged ~5
60 million years ago[17]. In culture at 39°C, *S. cerevisiae* doubled faster than *S. paradoxus* and
61 accumulated more biomass over a timecourse, a compound trait that we call thermotolerance.
62 The magnitude of differences in thermotolerance between species far exceeded that of strain
63 variation within each species (Figure 1), whereas no such effect was detectable at 28°C (Figure
64 S1). The failure by *S. paradoxus* to grow to high density at 39°C was, at least in part, a product
65 of reduced survival relative to that of *S. cerevisiae,* as cells of the former were largely unable to
66 form colonies after heat treatment (Figure S2). In microscopy experiments, *S. paradoxus* cells
67 were almost uniformly visible as large-budded dyads after 24 hours at 39°C (Figure S3),
68 suggestive of defects late in the cell cycle as a proximal cause of death[18]; no such tendency
69 was apparent in *S. cerevisiae* at high temperature, or in either species at 28°C (Figure S3).

70

71 **Massively parallel reciprocal hemizygosity testing by RH-seq**

72

73 We set out to dissect the genetic basis of *S. cerevisiae* thermotolerance, using a genomic
74 implementation of the reciprocal hemizygote test[12,13] (Figure 2A). For this purpose, we first
75 mated *S. cerevisiae* strain DBVPG1373, a soil isolate from the Netherlands, with *S. paradoxus*
76 strain Z1, an English oak tree isolate. The resulting sterile hybrid had a thermotolerance
77 phenotype between those of its purebred parents (Figure S4). In this hybrid background we
78 generated hemizygote mutants using a plasmid-borne, selectable PiggyBac transposon
79 system[19]. We cultured the pool of mutants in bulk for ~7 generations at 39°C and, separately, at
80 28°C. From cells in each culture we sequenced transposon insertion locations[20] as a readout of
81 the genotypes and abundance of mutant hemizygote clones present in the selected sample. In
82 these sequencing data, at each of 4888 genes we detected transposon mutant clones in both

species' alleles in the hybrid (Figure S5), with transposon insertions distributed in a largely unbiased manner across the genome (Figure S6). For a given gene, we tabulated the abundances of mutants whose transposon insertion fell in the *S. cerevisiae* allele of the hybrid, after high-temperature selection relative to the 28°C control, and we compared them to the abundance distribution of mutants in the *S. paradoxus* allele (Figure 2A). Any difference in abundance between these reciprocal hemizygote cohorts can be ascribed to variants between the retained alleles at the respective locus; we refer to the comparison as reciprocal hemizygosity analysis via sequencing (RH-seq). Integrating this approach with a quality-control pipeline (Figure S5), in a survey of 3416 high-coverage genes we identified 8 top-scoring hits (false discovery rate 0.01; Figure 2B). At each such locus, disruption of the *S. cerevisiae* allele in the hybrid was associated with low clone abundance after selection at 39°C relative to 28°C (Figure 2B), reflecting a requirement for the *S. cerevisiae* allele for thermotolerance. None of the genes mapped by RH-seq had a known role in the yeast heat shock or stress responses. All were annotated as housekeeping factors: *ESP1, DYN1, MYO1, CEP3, APC1,* and *SCC2* function in chromosome segregation and cytokinesis, and *AFG2* and *TAF2* in transcription/translation.

To evaluate the role in thermotolerance of genes that emerged from RH-seq, we first sought to verify that growth differences between hemizygotes at a given locus were the consequence of allelic variation and not an artifact of our genomic approach. As a complement to our analysis of transposon mutants, for each RH-seq hit gene we engineered hemizygotes by targeted deletion of each species' allele in turn in the hybrid. In growth assays, the strain lacking the *S. cerevisiae* allele at each gene grew poorly at high temperature (Figure 2B), with little impact at 28°C (Figure S7), consistent with fitness inferences from RH-seq. And in each case, the *S. paradoxus* allele made no contribution to the phenotype of the hybrid, since deleting it had no effect

108 (Figures 2B and S7). We conclude that the loci emerging from RH-seq represent bona fide
109 determinants of thermotolerance in the hybrid.
110
111 **Validation of RH-seq gene hits in purebreds**
112
113 We expected that variation at our RH-seq hits, though mapped by virtue of their impact in the
114 hybrid, could also explain thermotolerance differences between purebred species. As a test of
115 this notion, for each mapped gene in turn, we replaced the two copies of the endogenous allele
116 in each purebred diploid with the allele from the other species. Growth assays of these
117 transgenics established the *S. cerevisiae* allele of each locus as necessary or sufficient for
118 biomass accumulation at 39°C, or both: thermotolerance in the *S. cerevisiae* background was
119 compromised by *S. paradoxus* alleles at 7 of the 8 genes and, in *S. paradoxus*, improved by *S.*
120 *cerevisiae* alleles at 6 of 8 loci (Figure 3). Allele replacements had little impact on growth at
121 28°C (Figure S8). These trends mirrored the direction of locus effects from hemizygotes in the
122 hybrid, though the magnitudes were often different. Most salient were the small effect sizes in *S.*
123 *paradoxus* relative to other backgrounds, indicative of strong epistasis in this poorly-performing
124 species (Figure S9). Thus, the loci mapped by RH-seq in an interspecies hybrid contribute
125 causally to thermotolerance in purebreds, with effect sizes that depend on the context in which
126 they are interrogated.
127
128 Avid growth at high temperature is a defining characteristic of *S. cerevisiae* as a species,
129 relative to other Saccharomycetes (refs. 14-16 and Figure 1). In principle, the loci mapped by
130 RH-seq could be unique to the genetic architecture of thermotolerance in our focal *S. cerevisiae*
131 strain, DBVPG1373, or be part of a mechanism common to many *S. cerevisiae* isolates. In
132 support of the latter model, transgenesis experiments showed that a diverse panel of *S.*
133 *cerevisiae* isolates all harbored alleles conferring modest but significant growth benefits at high

134 temperature, and alleles from multiple *S. paradoxus* isolates were deleterious (Figure S10A-B).
135 We detected no such impact at 28°C (Figure S10A-B). Similarly, we found elevated sequence
136 divergence from *S. paradoxus* to be a shared feature of *S. cerevisiae* strains at the loci mapped
137 by RH-seq (using the absolute divergence measure D_{xy}; Figure S10C). These findings indicate
138 that the *S. cerevisiae* population accumulated divergent, pro-thermotolerance alleles at the loci
139 mapped by RH-seq, consistent with a role in the trait for these genes across the species.
140 Likewise, in the yeast phylogeny, RH-seq hit genes were distinguished by accelerated evolution
141 along the branch leading to *S. cerevisiae,* as expected if the ancestral program has been
142 conserved among the other species in the clade (Figure S10C).
143

144 ## Discussion

145

146 In this work, we have developed the RH-seq method for genome-wide mapping of natural trait
147 variation, and we have used it to elucidate the genetics of thermotolerance in reproductively
148 isolated yeasts. Growth at high temperature is likely a derived character in *S. cerevisiae*[14-16],
149 and the mechanism by which evolution built the trait, after the split from *S. paradoxus*, has
150 remained unknown. In pursuing the genetics of this putative ancient adaptation, we complement
151 studies of younger, intra-specific variants that erode thermotolerance, in the few *S. cerevisiae*
152 strains that have lost the trait relatively recently[12,21]. We have sought to shed light on more
153 ancient evolutionary events by considering *S. paradoxus* as a representative of the ancestral
154 state, to which thermotolerant *S. cerevisiae* can be compared.
155

156 Using this approach, we have mapped eight loci at which *S. cerevisiae* alleles are necessary
157 and sufficient for thermotolerance. Six of these genes are essential for growth in standard
158 conditions[22], and all eight contribute to fundamental growth processes. *ESP1, DYN1, CEP3,*

159 *APC1, MYO1,* and *SCC2* mediate mitotic spindle assembly, chromatid cohesion and separation,
160 cytokinesis, and mitotic exit; *AFG2* regulates the release of maturation factors from the
161 ribosome; and *TAF2* encodes a TFIID subunit. In each case, our growth experiments in the
162 interspecific hybrid have shown that the *S. paradoxus* allele acts as a hypomorph at high
163 temperature. Our work leaves unanswered exactly how heat-treated *S. paradoxus* cells die in
164 the absence of these functions, though their large-budded morphology strongly suggests
165 regulated arrest or stochastic failure late in the cell cycle. Given that some but not all RH-seq hit
166 loci have roles in mitosis, it is likely only one of the choke points at which *S. paradoxus* alleles
167 are a liability at high temperature. Assuming that these heat-sensitive alleles also littered the
168 genome of the common ancestor with *S. cerevisiae*, thermotolerance would have evolved along
169 the *S. cerevisiae* lineage by resolving each of them, boosting the heat resistance of many
170 housekeeping processes. Such a mechanism would dovetail with the recent finding that, across
171 species, the limiting temperature for cell growth correlates with the melting temperatures of a
172 subset of essential proteins[23].
173
174 These insights into the evolution of a complex yeast trait serve as a proof of concept for RH-
175 seq. To date, the reciprocal hemizygosity test has led to landmark discoveries in a candidate-
176 gene framework, confirming the effects of variation at a given locus identified by other
177 means[12,13]. Schemes to scale up the test have generated a genome's worth of hemizygotes
178 from deletion-strain purebreds, which tend to harbor secondary mutations that come through
179 screens as false positives[24,25]. As such, a key advantage of RH-seq is that we carry out
180 mutagenesis in the hybrid, which ensures coverage of essential genes and obviates the use of
181 mutation-prone null genotypes. Furthermore, any secondary mutations that do arise in a given
182 hemizygote clone should have little influence in RH-seq mapping, because deep mutagenesis
183 generates many independent clones per gene that are analyzed together. One important caveat
184 of RH-seq, as in single-gene reciprocal hemizygote tests, is the assumption that no epistasis

unique to the hybrid will mask the effects of loci underlying a trait difference of interest between the parents. In our case study, the genetic architecture of thermotolerance in the hybrid did bear out as relevant for the purebreds, albeit with locus effect sizes that varied across the backgrounds. More dramatic discrepancies may be particularly likely when the hybrid has a heterotic (*i.e.* extreme) phenotype and is a poor model for the genetics of the parents[26]. The choice of a non-heterotic hybrid in which to pursue RH-seq would be analogous to classical linkage mapping in a cross whose progeny have, on average, phenotypes that are intermediate between those of the parents.

In fact, although we have focused here on ancient divergence, the RH-seq method would be just as applicable to individuals within a species, as a high-resolution alternative to linkage analysis. We thus anticipate that RH-seq will accelerate the mapping of genotype to phenotype in many systems, whether the parents of a cross are closely related or members of a species complex that have been locally adapting for millions of years.

200 Figure 1

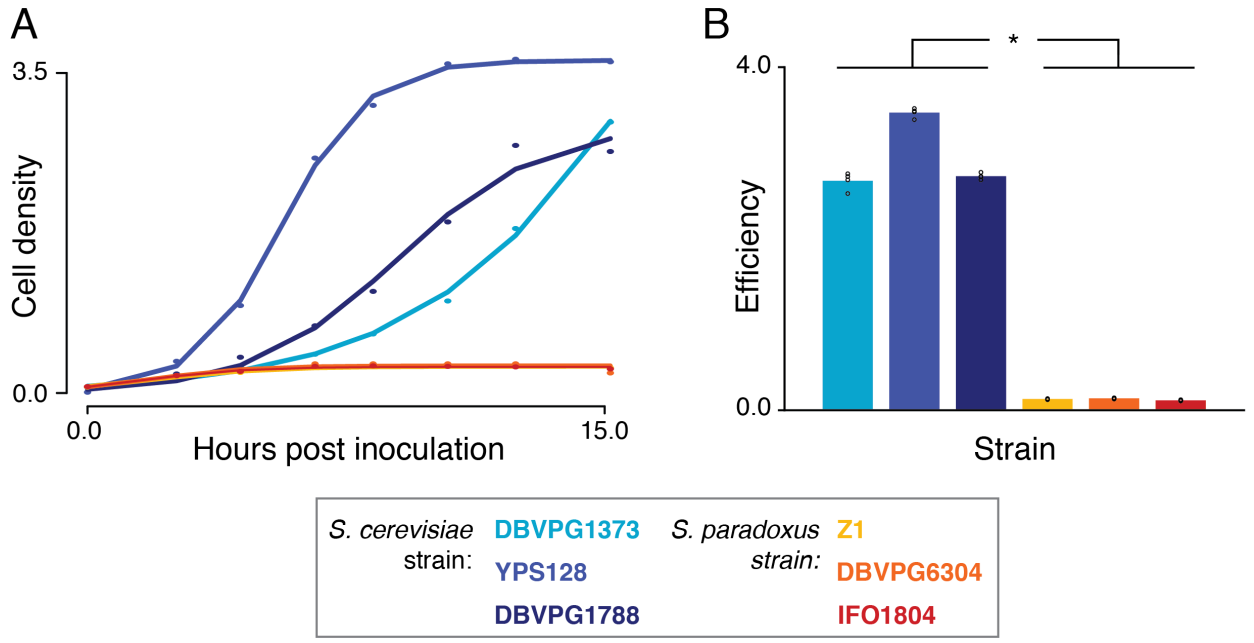

201

202 **Figure 1. *S. cerevisiae* grows better at high temperature than *S. paradoxus.***

203 **A**, Each point reports cell density (OD_{600}) of the indicated wild isolate of *S. cerevisiae* (blue) or

204 *S. paradoxus* (orange) over a timecourse of growth at 39°C. Each solid line shows a logistic

205 population growth model fit to the respective cell density measurements. **B**, Each bar reports

206 mean efficiency (n = 4) of the indicated strain at 39°C, defined as the difference between cell

207 density at 24 hours of growth and that at the time of inoculation. *, $p = 3.78 \times 10^{-11}$; individual

208 measurements are reported as open circles.

209

210

211

212

213 Figure 2

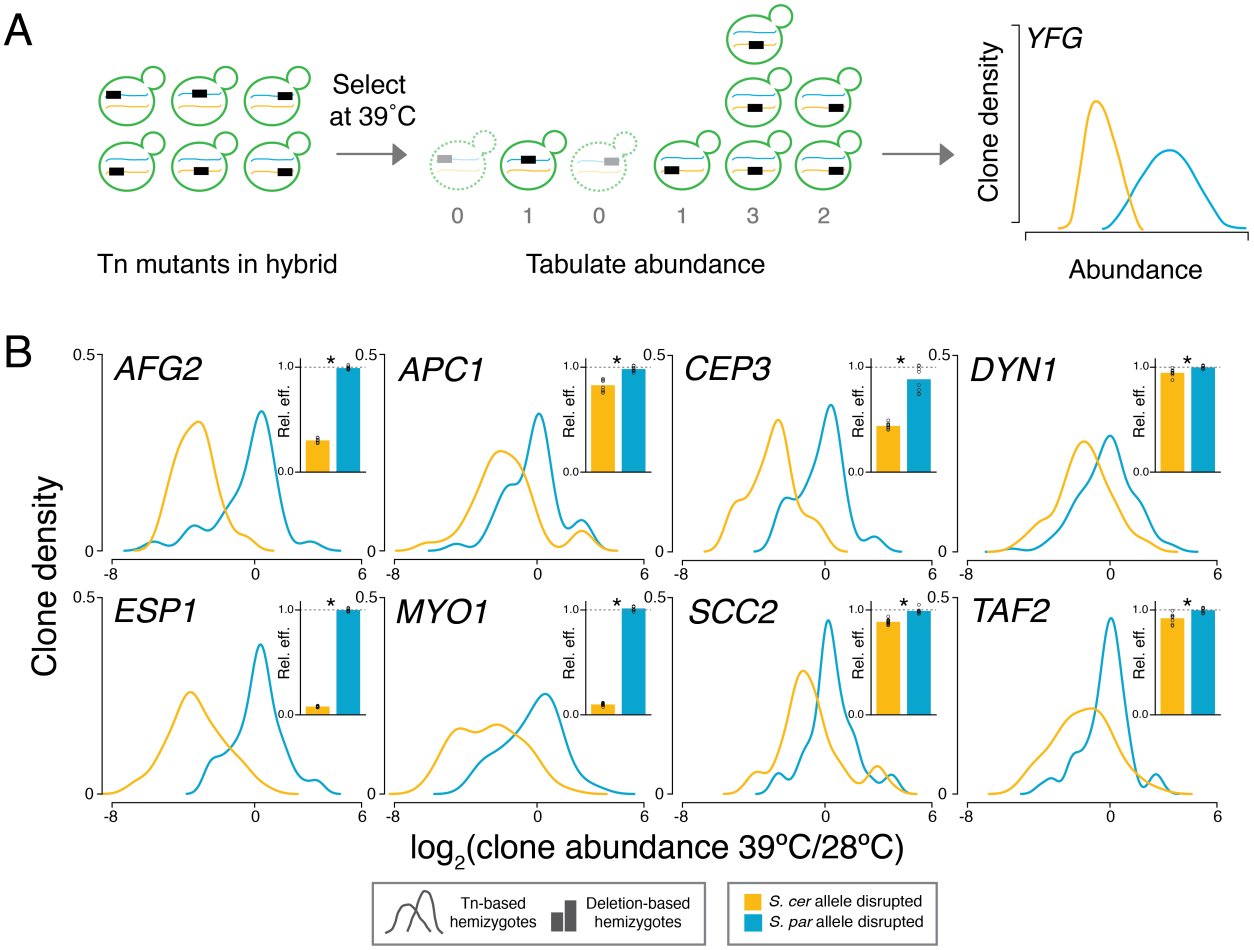

214

215 **Figure 2. Mapping thermotolerance by RH-seq.**

216 **A**, A transposon (rectangle) disrupts the allele from *S. cerevisiae* (blue) or *S. paradoxus*
217 (orange) of a gene (*YFG*) in an interspecific hybrid (green). Clones lacking the pro-
218 thermotolerance allele grow poorly at 39°C (dashed outlines), as measured by sequencing and
219 reported in smoothed histograms (traces, colored to indicate the species' allele that is not
220 disrupted). **B**, Each panel reports results from one RH-seq hit locus. In the main figure of a
221 given panel, the *x*-axis reports the $\log_2$ of abundance, measured by RH-seq after selection at
222 39°C, of a clone harboring a transposon insertion in the indicated species' allele, relative to the
223 analogous quantity for that clone from selection at 28°C. The *y*-axis reports the proportion of all
224 clones bearing insertions in the indicated allele that exhibited the abundance ratio on the *x*, as a

225 kernel density estimate. In insets, each bar reports the relative efficiency, calculated as the
226 mean growth efficiency at 39°C (n = 8-12) of the indicated targeted-deletion hemizygote
227 measured in liquid culture assays, normalized to the analogous quantity for the wild-type hybrid.
228 *, $p \leq 0.002$; individual measurements are reported as open circles.
229

230 Figure 3

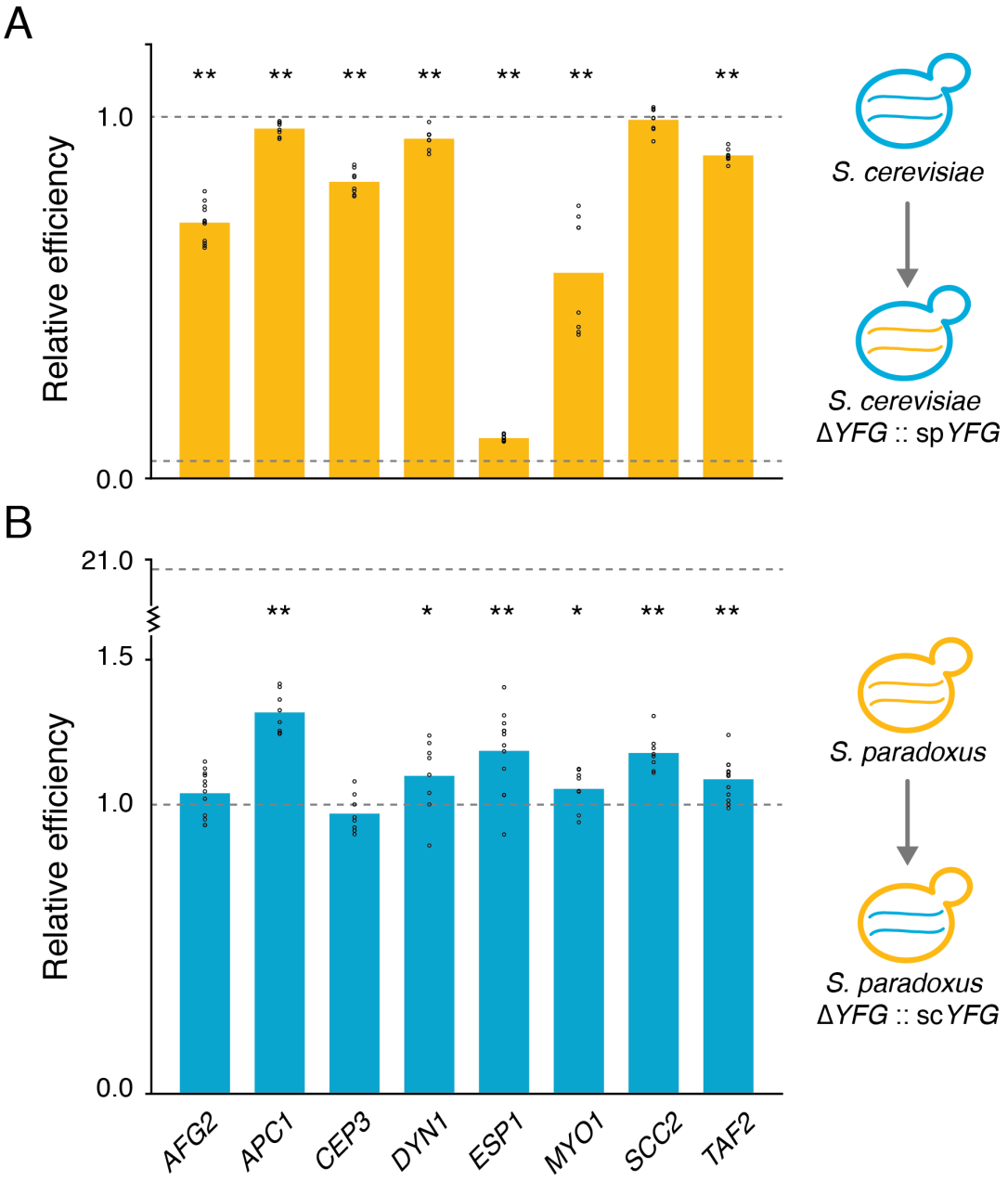

231

232 **Figure 3. *S. cerevisiae* thermotolerance alleles are necessary and sufficient for growth at**

233 **high temperature.**

234 **A**, Each bar reports mean growth efficiency at 39°C, measured in liquid culture assays (*n* = 6-

235 12), of an *S. cerevisiae* strain harboring the *S. paradoxus* allele at the indicated RH-seq hit

236 locus, relative to the analogous quantity for wild-type *S. cerevisiae*. **B**, Data are as in **A**, except

237 that each bar reports results from a *S. paradoxus* strain harboring the *S. cerevisiae* allele at the
238 indicated locus, normalized to wild-type *S. paradoxus*. In a given panel, the top and bottom
239 dotted lines report the relative efficiency of wild-type *S. cerevisiae* and *S. paradoxus*,
240 respectively. *, $p \leq 0.036$; **, $p \leq 0.001$. Individual measurements are reported as open circles.
241

242 # Materials and Methods

243

244 **Strains**

245

246 Strains used in this study are listed in Table S1. Homozygous diploid strains of *S. cerevisiae*
247 and *S. paradoxus* used as parents of the interspecific hybrid, and as the backgrounds for allele-
248 swap experiments, were homothallic DBVPG1373 and Z1, respectively. In the case of the
249 hybrid parents, each strain was rendered homozgyous null for *URA3* via homologous
250 recombination with a HYGMX cassette, then sporulated; a given mated spore from a dissected
251 tetrad was grown up into a diploid that was homozygous null at *URA3* and tested for the
252 presence of both genomes by PCR with species-specific primers.

253

254 **piggyBac transposon machinery**

255

256 For untargeted, genome-scale construction of reciprocal hemizygotes in the *S. cerevisiae* x *S.*
257 *paradoxus* hybrid, we adapted methods for piggyBac transposon mutagenesis[19] to develop a
258 system in which the transposon machinery was borne on a selectable and counter-selectable
259 plasmid lacking a centromere. We constructed this plasmid (final identifier pJR487) in three
260 steps. In step I we cloned the piggyBac transposase enzyme gene driven by the *S. cerevisiae*
261 *TDH3* promoter (from plasmid p3E1.2, a gift from Malcolm Fraser, Notre Dame) into plasmid
262 pJED104 (which contains *URA3*, an ARS, and the *CEN6* locus, and was a gift from John
263 Dueber, UC Berkeley). For this cloning, the amplification used a forward and reverse primer
264 containing a BamHI and XhoI site, respectively, that upon restriction digest yielded sticky ends
265 for ligation to recipient BamHI and XhoI sites in digested pJED104. We used the resulting
266 plasmid as input into step II, removal of the *CEN6* sequence: we first amplified the entire

267 plasmid with primers that initiated outside of *CEN6* and were directed away from it, and
268 contained reciprocally complementary NheI sites; sticky ends of the linear PCR product were
269 then ligated together for re-circularization. We used the resulting plasmid as input into step III,
270 the cloning in of a construct comprised of the KANMX cassette flanked by long terminal arms
271 (328bp and 361bp) from the piggyBac transposon. We first amplified KANMX from pUG6[27] and
272 each transposon arm from p3E1.2, using primers that contained overlapping sequence on the
273 fragment ends that would ultimately be the interior of the construct, and XbaI sites on the
274 fragment ends that would ultimately be the 5' and 3'-most ends of the construct. We stitched the
275 three fragments together by overlap extension PCR, digested the resulting construct and the
276 plasmid from step II with XbaI, and annealed sticky ends of the two to yield the final pJR487
277 plasmid.
278
279 **Untargeted hemizygote construction via transposon mutagenesis**
280
281 For mutagenesis, pJR487 was gigaprepped using a column kit (Zymo Research) to generate
282 ~11 mg plasmid. To prepare for transformation, JR507 (the *S. cerevisiae* DBVPG1373 x *S.*
283 *paradoxus* Z1 hybrid) was streaked from a -80°C freezer stock onto a yeast peptone dextrose
284 (YPD, 1% yeast extract [BD], 2% yeast peptone [BD], 2% D-glucose [Sigma]) agar plate and
285 incubated for 2 days at 26°C. A single colony was inoculated into 100 mL YPD and shaken at
286 28°C, 200rpm for ~24 hours. The next day, we transferred cells from this pre-culture, and YPD,
287 to each of four 1 L flasks at the volumes required to attain an optical density at 600 nm (OD_{600})
288 of 0.2 in 500 mL each. We cultured each for 6 hours at 28°C with shaking at 200rpm. Two of
289 these cultures were combined into 1 L of culture and two into a separate 1 L, and each such
290 culture was subjected to transformation (for a total of two transformations) as follows. The 1 L
291 was split into twenty 50-mL conical tubes. Each aliquot was centrifuged and washed with water
292 and then with 0.1 M lithium acetate (LiOAc, Sigma) mixed with 1X Tris-EDTA buffer (10 mM

293 Tris-HCl and 1.0 mM EDTA); after spin-down, to each tube was added a solution of 0.269 mg of
294 pJR487 mixed 5:1 by volume with salmon sperm DNA (Invitrogen), and then to each was added
295 3 mL of 39.52% polyethylene glycol, 0.12M LiOAc and 1.2X Tris-EDTA buffer (12 mM Tris-HCl
296 and 1.2 mM EDTA). Tubes were rested for 10 minutes at room temperature, then heat-shocked
297 in a water bath at 39°C for 26 minutes. Cells from all 20 tubes were then combined. We
298 transferred cells from this post-transformation culture, and YPD, to each of three 1 L flasks at
299 the volumes required to attain an OD_{600} of ~0.35-4 in 500 mL. Each such culture was recovered
300 by shaking at 28°C and 200 rpm for 2 hours. G418 (Geneticin, Gibco) was added to each at a
301 concentration of 300 µg/mL to select for those cells which had taken up the plasmid, and
302 cultures were incubated with 200 rpm shaking at 28°C for two days until each reached an OD_{600}
303 of ~2.3. All six such selected cultures across the two transformations were combined. We
304 transferred cells from this combined culture, and YPD + G418 (300 ug/mL), to each of two 1 L
305 flasks at the volumes required to attain an OD_{600} of 0.2 in 500 mL each. We cultured each flask
306 at 28°C and 200 rpm shaking overnight until reaching an OD_{600} of 2.18 and combined the two
307 cultures again to yield one culture. To cure transformants of the pJR487 URA+ plasmid, we
308 spun down a volume of this master culture and resuspended in water with the volume required
309 to attain a cell density of 1.85 OD_{600} units/mL. 12 mL of this resuspension were plated (1 mL per
310 24.1cm x 24.1cm plate) onto plates containing complete synthetic media with 5-fluoroorotic acid
311 (5-FOA) [0.2% drop-out amino acid mix without uracil or yeast nitrogen base (YNB) (US
312 Biological), 0.005% uracil (Sigma), 2% D-glucose (Sigma), 0.67% YNB without amino acids
313 (Difco), 0.075% 5-FOA (Zymo Research)]. After incubation at 28°C to enable colony growth,
314 colonies were scraped off all 12 plates and combined into water at the volume required to attain
315 40 OD_{600} units per 900 µL, yielding the final transposon mutant hemizygote pool. This was
316 aliquoted into 1 mL volumes with 10% DMSO and frozen at -80°C.
317
318 **Thermotolerance phenotyping via selection of the hemizygote pool**

319

320 One aliquot of the pool of transposon mutant hemizygotes in the JR507 *S. cerevisiae*
321 DBVPG1373 x *S. paradoxus* Z1 hybrid background was thawed and inoculated into 150 mL of
322 YPD in a 250 mL flask, and cultured for 7.25 hours at 28°C, with shaking at 200 rpm. We used
323 this timepoint as time zero of our thermotolerance experiment, and took four aliquots of 6.43 mL
324 (7 OD units) as technical replicates for sequencing of transposon insertion positions (see
325 below). 9.19 mL of the remaining culture was back-diluted to an OD_{600} of 0.02 in a total of 500
326 mL YPD in each of six 2L glass flasks for cultures that we call selections; three were grown at
327 28°C and three at 39°C (shaking at 200 rpm) until an OD_{600} of 1.9-2.12 was reached,
328 corresponding to about 6.5 doublings in each case. Four cell pellets of 7 OD_{600} units each were
329 harvested from each of these biological replicate flasks, for sequencing as technical replicates
330 (see below). In total, 28 pellets were subjected to sequencing: 4 technical replicates from the
331 time-zero culture; 3 biological replicates, 4 technical replicates each, from the 28°C selection;
332 and 3 biological replicates, 4 technical replicates each, from the 39°C selection.

333

334 **Tn-seq library construction**

335

336 To determine the abundance of transposon mutant hemizygote clones after selection, we first
337 sequenced transposon (Tn) insertions as follows. Each cell pellet from a time zero or selection
338 sample (see above) was thawed on ice, and its genomic DNA (gDNA) was harvested with the
339 ZR Fungal/Bacterial DNA MiniPrep kit (Zymo Research). gDNA was resuspended in DNA
340 elution buffer (Zymo) pre-warmed to 65°C and its concentration was quantified using a Qubit 3.0
341 fluorometer. Illumina Tn-seq library construction was as described[28]. Briefly, gDNA was
342 sonicated and ligated with common adapters, and for each fragment deriving from a Tn insertion
343 in the genome, a sequence containing a portion of the transposon and a portion of its genomic
344 context (the Tn-genome junction) was amplified using one primer homologous to a region in the

345 transposon, and another primer homologous to a region in the adapter. The indexed adapter-
346 specific primer was
347 CAAGCAGAAGACGGCATACGAGATNNNNNNGTGACTGGAGTTCAGACGTGTGCTCTTCCG
348 ATCT, where the six N's are a unique index used for multiplexing multiple libraries onto the
349 same Hiseq sequencing lane, and the transposon specific primer was
350 ATGATACGGCGACCACCGAGATCTACACTCTTTCCCTACACGACGCTCTTCCGATCT
351 NNNNNNAGCAATATTTCAAGAATGCATGCGTCAAT, where N's are random nucleotides.
352 Amplification used Jumpstart polymerase (Sigma) and the following cycling protocol: 94°C-2
353 min, [94°C-30 sec, 65°C-20 sec, 72°C-30 sec] X 25, 72°C-10 min. Sequencing of single-end
354 reads of 150 bp was done over eight lanes on a HiSeq 2500 at the Joint Genome Institute
355 (Walnut Creek, CA). Reads sequenced per library are reported in Table S2.
356
357 **Tn-seq read-mapping and data analysis**
358
359 For analysis of data from the sequencing of Tn insertion sites in pools of hemizygotes, we first
360 searched each read for a string corresponding to the last 20 base pairs of the left arm of the
361 piggyBac transposon sequence, allowing up to two mismatches. For each Tn-containing read,
362 we then identified the genomic location of the sequence immediately downstream of the Tn
363 insertion site, which we call the genomic context of the insertion, by mapping with BLAT
364 (minimum sequence identity = 95, tile size = 12) against a hybrid reference genome made by
365 concatenating amended *S. cerevisiae* DBVPG1373 and *S. paradoxus* Z1 genomes (see below).
366 These genomic-context sequence fragments were of variable length; any case in which the
367 sequence was shorter than 50 base pairs was eliminated from further analysis, as was any case
368 in which a genomic-context sequence mapped to more than one location in the hybrid
369 reference. The resulting data set thus comprised reads containing genomic-context sequences
370 specifically mapping to a single location in either *S. cerevisiae* DBVPG1373 or *S. paradoxus* Z1,

371 which we call usable reads. For a given library, given a cohort of usable reads whose genomic-
372 context sequence mapped to the same genomic location, we inferred that these reads
373 originated from clones of a single mutant with the Tn inserted at the respective site, which we
374 call an insertion. In cases where the genomic-context sequences from reads in a given library
375 mapped to positions within 3 bases of each other, we inferred that these all originated from the
376 same mutant genotype and combined them, assigning to them the position corresponding to the
377 single location to which the most reads mapped among those combined. For a given insertion
378 thus defined, we considered the number of associated reads n_{insert} as a measure proportional to
379 the abundance of the insertion clone in the cell pellet whose gDNA was sequenced. To enable
380 comparison of these abundances across samples, we tabulated the total number of usable
381 reads n_{pellet} from each cell pellet, took the average of this quantity across pellets, $<n_{pellet}>$, and
382 multiplied each n_{insert} by $<n_{pellet}>/ n_{pellet}$ to yield a_{insert}, the final normalized estimate of the
383 abundance of the insertion clone in the respective pellet. For any insertions that were not
384 detected in a given pellet's library ($n_{insert} = 0$) but detectable in another library of the data set, we
385 assigned $n_{insert} = 1$.
386
387 We evaluated, from the mapped genomic-context sequence of each insertion, whether it fell into
388 a gene according to the *S. cerevisiae* and *S. paradoxus* genome annotations[17,29], and we
389 retained for further analysis only those insertions that fell into genes that were syntenic in the
390 two species. For each such insertion, for each biological replicate corresponding to a selection
391 culture (at 28°C or 39°C), we averaged the normalized abundances a_{insert} across technical
392 replicates, yielding a single abundance estimate $<a_{insert}>_{technical}$ for the biological replicate. We
393 then calculated the mean of the latter quantities across all biological replicates of the selection,
394 to yield a final abundance estimate for the insertion in this selection, $<a_{insert}>_{total}$. Likewise, for
395 each insertion and selection experiment we calculated $CV_{insert,total}$, the coefficient of variation of
396 $<a_{insert}>_{technical}$ values across biological replicates.

397

398 To use Tn-seq data in reciprocal hemizygosity tests, we considered for analysis only genes
399 annotated with the same (orthologous) gene name in the *S. cerevisiae* and *S. paradoxus*
400 reference genomes. For each insertion, we divided the $\langle a_{insert} \rangle_{total}$ value from the 39°C selection
401 by the analogous quantity from the 28°C selection and took the $\log_2$ of this ratio, which we
402 consider to reflect thermotolerance as measured by RH-seq. For each gene in turn, we used a
403 two-tailed Mann-Whitney U test to compare thermotolerance measured by RH-seq between the
404 set of insertions falling into the *S. cerevisiae* alleles of the gene, against the analogous quantity
405 from the set of insertions falling into the *S. paradoxus* allele of the gene, and we corrected for
406 multiple testing using the Benjamini-Hochberg method.
407

408 We tabulated the number of inserts and genes used as input into the reciprocal hemizygote test,
409 and the number of top-scoring genes emerging from these tests, under each of a range of
410 possible thresholds for coverage and measurement noise parameter values (Figure S5). We
411 used in the final analysis the parameter-value set yielding the most extensive coverage and the
412 most high-significance hits: this corresponded to insertions whose abundances had, in the data
413 from at least one of the two selections (at 28°C or 39°C), $CV_{insert,total} \leq 1.5$ and $\langle a_{insert} \rangle_{total} \geq 1.1$,
414 and genes for which this high-confidence insertion data set contained at least 5 insertions in
415 each species' allele. This final data set comprised 110,678 high-quality insertions (Table S3) in
416 3416 genes (Table S4).
417

418 **Amended reference genome construction**

419

420 We generated reference genomes for *S. cerevisiae* strain DBVPG1373 and *S. paradoxus* strain
421 Z1 as follows. Raw genome sequencing reads for each strain were downloaded from the
422 SGRP2 database (ftp://ftp.sanger.ac.uk/pub/users/dmc/yeast/SGRP2/input/strains). Reads were

423 aligned using bowtie2[30] with default options; DBVPG1373 reads were aligned to version
424 R64.2.1 of the reference sequence of the *S. cerevisiae* type strain S288C (Genbank Assembly
425 Accession GCA_000146045.2), and Z1 reads were aligned to the *S. paradoxus* strain CBS432
426 reference sequence[31]. Single nucleotide variants (SNPs) were called using a pipeline of
427 samtools[32], bcftools and bgzip, and were filtered for a quality score (QUAL) of >20 and a
428 combined depth (DP) of >5 and either <65 (*S. cerevisiae*) or <255 (*S. paradoxus*). We then
429 amended each reference genome with the respective filtered SNPs: we replaced the S288C
430 allele with that of DBVPG1373 at each filtered SNP using bcftools' consensus command with
431 default options (42,983 base pairs total), and amendment of the CBS432 sequence was carried
432 out analogously using Z1 alleles (15,126 base pairs total).
433
434 **Targeted-deletion hemizygote construction by homologous recombination**
435
436 A given targeted hemizygote for each RH-seq hit gene except *TAF2* was generated in the *S.*
437 *cerevisiae* DBVPG1373 x *S. paradoxus* Z1 hybrid (JR507) by knocking out the allele of the gene
438 from one species via homologous recombination with KANMX as described[33] with 70 base pairs
439 of homology on the 5' and 3' ends of the cassette; checking was via diagnostic PCR. Two or
440 more independent transformants were isolated and phenotyped for each hemizygote genotype
441 (Table S1).
442
443 **Construction of allele replacement and targeted hemizgyote strains with Cas9**
444
445 At each RH-seq hit gene, we constructed strains in wild-type homozygous diploid *S. cerevisiae*
446 DBVPG1373 in which both copies of the endogenous allele were replaced by the allele from an
447 *S. paradoxus* isolate (Z1 for Figures 3, S8, and S9, and other strains as indicated for Figure
448 S10), and likewise for replacement of alleles from *S. cerevisiae* (DBVPG1373 in Figures 3, S8,

449 and S9, and other strains as indicated for Figure S10) into *S. paradoxus* Z1. We call each such
450 strain an allele-replacement strain, and each was constructed using a dual-guide Cas9
451 transgenesis method[34] in which a linear PCR fragment from the donor species is incorporated
452 into the recipient genome by homology-directed repair of two chromosomal double-strand
453 breaks induced by Cas9. Briefly, for each allele of each gene, we designed two guide RNAs for
454 double-strand breaks by Cas9: one guide targeted a position ~1000 base pairs 5' to the coding
455 start or at the 3' end of the closest upstream gene, whichever was closer, and the other guide
456 targeted the region of the coding stop. The precise cut site of each was chosen to contain an
457 NGG immediately downstream of variants between the *S. cerevisiae* and *S. paradoxus* strains,
458 to avoid re-cutting of the donor allele by Cas9 after it had been introduced into the recipient
459 strain. We cloned the two guide RNAs, a KANMX cassette, and the gene encoding the *S.*
460 *pyogenes* Cas9 protein into a single plasmid as described[34]. The resulting plasmid was
461 propagated in DH5a *E. coli* and miniprepped with a column miniprep kit (Qiagen). Separately, to
462 generate the fragment to be used as the donor for DNA repair after Cas9 cutting, we PCR-
463 amplified the respective region from the donor strain, with primers whose 5'-most 70 base pairs
464 were homologous to the recipient and whose 3'-most 20 base pairs were homologous to the
465 donor, except in the case of transgenesis using *S. cerevisiae* donors other than DBVPG1373 or
466 *S. paradoxus* donors other than Z1 (for Figure S10), for which the 3'-most 20 base pairs were
467 homologous to DBVPG1373 or Z1, respectively. The homology region at the 5' end of the gene
468 ended at most 31 base pairs upstream of the 5' cut site, and the homology region at the 3' end
469 of the gene started at most 33 base pairs downstream of the 3' cut site. The donor fragment
470 product was purified with a column kit (Qiagen) and ethanol-precipitated. We then
471 simultaneously transformed, using the lithium acetate method, the donor fragment and dual-
472 guide Cas9 plasmid into the recipient strain, using donor:acceptor ratios of 0.38:10 to 1:5, with
473 0.5-26 ug of plasmid. In this transformation, heat shock was for 20-30 minutes at 39-42°C in
474 transformations of *S. cerevisiae* DBVPG1373, and 10-20 minutes at 37-39°C for transformations

475 of *S. paradoxus* Z1. Transformants were plated on YPD+G418 (300 µg/mL) to select for cells
476 that retained the plasmid. From this selection we patched single colonies onto YPD without
477 G418, under the expectation that by the time a lawn came up for each patch, its cells would
478 have lost the Cas9 plasmid. Each such strain was Sanger-sequenced at the junctions of the
479 recipient and donor sequence. Positive patches were streaked to single colonies on YPD plates,
480 and cells from each such colony were used to inoculate a patch on a YPD plate and, separately,
481 to inoculate a patch on a YPD+G418 plate. Those colonies whose patches grew on the former
482 but not on the latter were inferred to be cured of the plasmid and stored at -80°C. For all genes
483 except *DYN1*, 2-3 such strains from each transformation were retained for thermotolerance
484 assays and underwent Sanger sequencing of the entire locus to determine the exact swapped
485 region (Table S1). For *DYN1* allele-replacement in *S. paradoxus* Z1, the Cas9-based strategy
486 yielded a single verified clone in which the *S. paradoxus* Z1 allele of *DYN1* was replaced by that
487 of *S. cerevisiae* DBVPG1373, and likewise for *DYN1* allele-replacement in *S. cerevisiae*
488 DBVPG1373. In each case, we mated the single swap clone to a wild-type of the respective
489 species background, confirmed heterozygosity of the resulting diploid via allele-specific
490 diagnostic PCR at the *DYN1* locus, sporulated, and dissected tetrads, allowing each spore to
491 autodiploidize and grow up as a homozygote; we retained from one such tetrad the two spores
492 that were homozygous at the *DYN1* locus for the swapped allele, as confirmed by sequencing,
493 and stored these at -80°C.
494
495 Targeted-deletion hemizygote strains for *TAF2* were generated by knocking out the *S.*
496 *cerevisiae* or the *S. paradoxus* allele in the interspecific hybrid (JR507) using the above
497 methods for Cas9 cutting and repair, with the following differences. To generate the fragment to
498 be used as the donor for DNA repair after Cas9 cutting, we PCR-amplified the NATMX cassette
499 from pBC713 (a gift from John Dueber, constructed as in [35]) using primers whose 5'-most 70
500 base pairs were homologous to the recipient and whose 3'-most 20 base pairs were

homologous to the cassette. The homology region at the 5' end of the gene ended 22 base pairs outside the 5' cut site (which was upstream of coding start), and the homology region at the 3' end of the gene started 33 base pairs outside the 3' cut site. Positive strains were confirmed by PCR. Two independent transformants were isolated and phenotyped for each genotype (Table S1).

Growth assays

Growth measurements of wild-type SGRP strains.

For the growth timecourse of a given wild-type, purebred homozygote isolate from the SGRP collection at 28°C, it was streaked from a -80°C freezer stock onto a YPD agar plate and incubated at 26°C for 3 days. A single colony was inoculated into liquid YPD and grown for 24 hours at 28°C with shaking at 200 rpm. This culture was back-diluted into YPD at an OD_{600} of ~0.05 and grown for an additional 5.5 hours at 28°C, 200 rpm, until reaching logarithmic phase. We transferred cells from each such pre-culture, and YPD, to each of 11 replicate wells of a 96-well plate, with volumes sufficient to yield a total volume of 150 µL per well at an OD_{600} of 0.02. The plate was covered with a gas-permeable membrane (Sigma) and incubated with orbital shaking in an M200 plate reader (Tecan, Inc.) at 28°C for 24 hours. For curves in Figure S1A, measurements for optical density at 595nm (OD_{595}) were taken every 30 minutes and for each timepoint, the average was taken across replicate wells. To subtract background OD_{595} for the resulting curve, we tabulated the mean of the five lowest values from all datapoints, excluding the first two, and subtracted this value from that of each timepoint, setting any negative value to 0. To smooth the resulting curve, we first replaced each timepoint measurement by its average with those of the timepoints immediately before and after it; then, for any timepoint whose measurement was not greater than or equal to the previous one, we set it to be equal to that

527 previous data point. For Figure S1B, the efficiency for a given growth curve (from a single well)
528 was calculated as the difference between the OD_{595} measured at the last four smoothed and
529 averaged data points and that of the first four smoothed and averaged data points. Efficiencies
530 from all of the wells from every *S. cerevisiae* isolate were combined and compared to
531 efficiencies from all of the wells for every *S. paradoxus* isolate in a two-sample two-tailed *t*-test.
532
533 For the growth timecourse of a given SGRP strain at 39°C (Figure 1A), we used a large-volume
534 flask growth paradigm to avoid the influence of plate effects on growth measurements at high
535 temperature in the incubated microplate reader, as follows. Each strain was streaked from a -
536 80°C freezer stock onto a YPD agar plate and incubated at 26°C for 3 days. A single colony of a
537 given strain was inoculated into liquid YPD and grown for 24 hours at 28°C with shaking at 200
538 rpm. Each of these cultures was back-diluted into YPD at an OD_{600} of 0.05 and grown for an
539 additional 5.5-7.5 hours at 28°C, shaking at 200 rpm, until reaching logarithmic phase. We
540 transferred cells from each such pre-culture, and YPD, to a glass 250 mL flask at the volumes
541 required to attain an OD_{600} of 0.05 in 100 mL YPD, and incubated it at 39°C with shaking at 200
542 rpm. OD_{600} readings were taken every ~2 hours for ~18 hours. Figure 1A reports representative
543 data from one of three such independent timecourse experiments. For curve fits, we used the
544 getInitial and SSlogis functions in R to estimate starting values for the parameters of the logistic
545 equation, and the nls function to fit the final parameters.
546
547 For efficiency measurements of a given SGRP isolate at 39°C in the large-volume format
548 (Figure 1B), it was streaked from a -80°C freezer stock onto a YPD agar plate and incubated at
549 26°C for 3 days. Two single colonies of each isolate were each inoculated into liquid YPD and
550 grown for 24 hours at 28°C with shaking at 200 rpm to generate two replicate pre-cultures. Each
551 was back-diluted into YPD at an OD_{600} at 600 nm of 0.05 and grown for an additional 5.5 hours
552 at 28°C, shaking at 200 rpm, until reaching logarithmic phase. The two pre-cultures were each

553 again back-diluted into YPD in 1-inch diameter glass tubes with a target OD_{600} of 0.05; the
554 actual OD_{600} of each was measured, after which it was grown at 39°C with shaking at 200rpm
555 for 24 hours, and OD_{600} was measured again. The efficiency for each replicate was calculated
556 as the difference between these final and initial OD_{600} values. The pipeline from inoculation off
557 solid plates through pre-culture, two back-dilutions, and growth at 39°C we refer to as a day's
558 growth experiment. For each day's experiments, we calculated the average efficiency across
559 the replicates of each isolate $<e_{strain}>$. We carried out two days' worth of replicate growth
560 experiments for each isolate. For a given species, we used the complete cohort of
561 measurements of $<e_{strain}>$ from all isolates of each species, across all days, as input into a two-
562 sample, two-tailed *t*-test to evaluate whether the suite of e_{strain} values across isolates of *S.*
563 *cerevisiae* was significantly different from the analogous set of values from *S. paradoxus*.
564
565 *Growth measurements of targeted-deletion hemizygotes and allele-replacement strains at 28°C.*
566
567 For efficiency measurements of a given targeted-deletion hemizygote or allele-replacement
568 strain at 28°C (Figures S7, S8 and S10), pre-culture and plate reader assays were as for wild-
569 type SGRP strains, except that 6 or more replicate wells were cultured per strain. 2-3
570 independently isolated targeted-deletion hemizygotes or allele-replacement strains (Table S1)
571 were assayed for each genotype. Each timecourse of targeted-deletion hemizygote or allele-
572 replacement strains also included the wild-type hybrid (JR507) or parent (*S. cerevisiae*
573 DBVPG1373 or *S. paradoxus* Z1), respectively, with pre-culture and replication as above.
574 Efficiency for a given growth curve (from a single well) was calculated as the difference between
575 the OD_{600} measured at the last four smoothed and averaged datapoints and that of the first four
576 smoothed and averaged datapoints, with smoothing and averaging as detailed above. For
577 Figure S7, relative efficiency for a given well of a given targeted-deletion hemizygote strain at
578 28°C was tabulated as its efficiency divided by that of the average of all replicate wells of the

579 wild-type hybrid (JR507) grown in the same experiment. For a given gene, we used the
580 complete cohort of these measurements, from all isogenic hemizygotes, as input into a two-
581 sample, two-tailed *t*-test to evaluate whether the relative efficiency of the strain in which the *S.*
582 *cerevisiae* allele was knocked out was lower than the analogous quantity from the strain in
583 which the *S. paradoxus* allele was knocked out. In Figures S8 and S10, allele-replacement
584 strains for a given gene were analyzed analogously, with the relative efficiency calculated
585 against the respective wild-type parent, and with a one-sample, two-tailed *t*-test to evaluate
586 whether the relative efficiency was significantly different from 1.
587
588 *Growth measurements of targeted-deletion hemizygotes and allele-replacement strains at 39°C.*
589
590 For efficiency measurements of a given targeted-deletion hemizygote strain at 39°C in the large-
591 volume format (Figure 2B), each strain was streaked from a -80°C freezer stock onto a YPD
592 agar plate and incubated at 26°C for 3 days. Two single colonies of a given strain were each
593 inoculated into liquid YPD and grown for 24 hours at 28°C with shaking at 200 rpm. Each such
594 pre-culture at stationary phase, or a log-phase outgrowth of it (which we used in the case of
595 *DYN1* and *TAF2*: the pre-culture and YPD were added at the volumes required to attain an
596 OD_{600} of 0.05 and grown for an additional 5.5 hours at 28°C, shaking at 200 rpm, until the
597 culture reached logarithmic phase) was used to inoculate YPD in 1-inch diameter glass culture
598 tubes with a target cell density corresponding to an OD_{600} of 0.05. The actual OD_{600} of each was
599 measured, after which it was grown at 39°C with shaking at 200 rpm for 24 hours, and OD_{600}
600 was measured again. The efficiency for each such replicate was then calculated as the
601 difference between the final and initial OD_{600} values. The pipeline from inoculation off solid
602 plates through pre-culture, back-dilution, and growth at 39°C we refer to as a day's growth
603 experiment for a targeted-deletion homozygote. In each such experiment, 2-3 independently
604 isolated targeted-deletion hemizygotes of a given gene in each direction were all assayed on

605 the same day, alongside the wild-type hybrid parent (JR507) with replicate structure and
606 methods as above. From each day's experiments, we calculated the average efficiency across
607 the replicates of the wild-type hybrid $<e_{hybrid}>$, and we used this quantity to normalize the
608 efficiency $e_{hemizyg}$ measured for each replicate of each hemizygote strain assayed on that day.
609 Thus, the final observable used for analysis for each replicate on a given day was
610 $e_{hemizyg}/<e_{hybrid}>$. We carried out 2-3 days' replicate growth experiments for each gene's
611 hemizygotes. For a given gene, we used the complete cohort of these measurements of
612 $e_{hemizyg}/<e_{hybrid}>$, from all days and all isogenic hemizygotes, as input into a two-sample, one-
613 tailed *t*-test to evaluate whether $e_{hemizyg}/<e_{hybrid}>$ of the strain in which the *S. cerevisiae* allele
614 was knocked out was lower than the analogous quantity from the strain in which the *S.*
615 *paradoxus* allele was knocked out.
616
617 For growth measurements of a given allele-replacement strain at 39°C in the large-volume
618 format (Figure 3, S7, S8 and S10), each strain was streaked from a -80°C freezer stock onto a
619 YPD agar plate and incubated at 26°C for 3 days. 1-2 single colonies of each strain were each
620 inoculated into liquid YPD and grown for 24 hours at 28°C with shaking at 200 rpm to generate
621 1-2 replicate pre-cultures. Each was back-diluted into YPD at an OD_{600} of 0.05 and grown for an
622 additional 5.5 hours at 28°C, shaking at 200 rpm, until reaching logarithmic phase. Each pre-
623 culture were each again back-diluted into YPD in 1-inch diameter glass tubes with a target
624 OD_{600} of 0.05 (for experiments using a single pre-culture, it was now split into two replicate pre-
625 cultures, each of the same OD_{600}); the actual OD_{600} of each was measured, after which it was
626 grown at 39°C with shaking at 200rpm for 24 hours, and OD_{600} was measured again. The
627 efficiency for each replicate was calculated as the difference between these final and initial
628 OD_{600} values. The pipeline from inoculation off solid plates through pre-culture, two back-
629 dilutions, and growth at 39°C we refer to as a day's growth experiment for an allele-swap strain.
630 In each such experiment, 2-3 independently isolated allele-swap strains targeting a given gene

631 in a given background were all assayed on the same day, alongside the respective wild-type
632 background strain (*S. cerevisiae* DBVPG1373 or *S. paradoxus* Z1) with replicate structure and
633 methods as above. For each day's experiments, we calculated the average efficiency across the
634 replicates of the wild-type parent $<e_{parent}>$, and we used this quantity to normalize the efficiency
635 e_{swap} measured for each replicate assayed on that day of each allele-swap strain in the
636 respective background. Thus, the final measurement used for analysis for each replicate on a
637 given day was $e_{swap}/<e_{parent}>$. We carried out 2-3 days' worth of replicate growth experiments for
638 each gene's allele-swap strains. For a given gene in a given background, we used the complete
639 cohort of measurements of $e_{swap}/<e_{parent}>$ from all days and all allele-swap strains as input into a
640 one-sample, one-tailed *t*-test to evaluate whether $e_{swap}/<e_{parent}>$ was significantly different from
641 1. For swaps of the *S. cerevisiae* allele of a given gene into *S. paradoxus*, we tested whether
642 $e_{swap}/<e_{parent}>$ was greater than 1 (*i.e.* that the swap strain grew better at 39°C than did its
643 parent), and for swaps of the *S. paradoxus* allele of a given gene into *S. cerevisiae*, we tested
644 whether $e_{swap}/<e_{parent}>$ was less than 1 (*i.e.* that the swap strain grew worse at 39°C than its
645 parent).
646
647 *Testing survival of wild-type parent strains at 39°C.*
648
649 To test the survival of heat-treated *S. paradoxus* Z1 and *S. cerevisiae* DBVPG1373 (Figure S2),
650 each strain was streaked from -80°C freezer stocks onto YPD agar plates and incubated at
651 26°C for 3 days. 1-2 single colonies of each parent were inoculated into liquid YPD and grown
652 for 24 hours at 28°C with shaking at 200 rpm to create 1-2 replicate pre-cultures. After 24 hours,
653 we transferred cells from each pre-culture, and YPD, to each of 2-4 tubes at the volumes
654 required to attain an OD_{600} of 0.05 in 11 mL YPD. Two tubes were incubated at 28°C and two at
655 39°C, all with shaking at 200 rpm for 24 hours. OD_{600} of each was measured; for each culture
656 grown at 28°C, 100 µL of a 1.0×10^{-5} serial dilution was plated to YPD, and for cultures grown at

657 39°C, *S. paradoxus* and *S. cerevisiae* were serially diluted to 10^{-1} and 5.0×10^{-5}, respectively.
658 Plates were incubated at 26°C for three days until single colonies appeared. Colonies on each
659 plate were counted, from which we tabulated the colony forming units per mL of culture plated,
660 and normalized by the optical density of the original plated culture. The pipeline from pre-culture
661 through treatment and colony counting we refer to as one day's worth of experiments. We used
662 the results of two days' worth of experiments (a total of four for each species and temperature)
663 as input into an ANOVA with species and temperature as factors, and took the *p*-value for the
664 interaction between the factors as the estimate of the significance of the difference between
665 species in the effect of temperature (of the 24-hour liquid culture) on cells' ability to grow into
666 colonies (at the permissive temperature).
667
668 **Microscopy and quantification**
669

670 For microscopy of *S. cerevisiae* DBVPG1373 and *S. paradoxus* Z1 (Figure S3), each species
671 was streaked from a -80°C freezer stock onto a YPD agar plate and incubated at 26°C for 3
672 days. Two single colonies of each strain were each inoculated into liquid YPD and grown for 24
673 hours at 28°C with shaking at 200 rpm to generate two replicate pre-cultures. Each was then
674 back-diluted into YPD at an OD_{600} of 0.05; one was grown at 39°C with shaking at 200rpm for
675 24 hours, and the other was grown at 28°C with shaking at 200rpm for 24 hours. After the 24
676 hour growth period, 0.5 OD units of each culture were harvested through centrifugation and
677 incubated in 66.5% ethanol for 1-4 hours at room temperature. Each sample was washed twice
678 with 1X Dulbecco's Phosphate Buffered Saline (DPBS, Gibco), resuspended in 0.5 mL of 1X
679 DPBS, and vortexed for 15 seconds on high. 5 µL of each sample was transferred to an
680 agarose pad made with 1% agarose and YPD. We observed samples on a Zeiss Axio Observer
681 inverted bright-field microscope at 100X magnification. Images were taken using a Hamamatsu

682 ORCA-Flash4.0 digital camera and visualized using ZEN software for image analysis. The
683 exposure of each image was set automatically through ZEN, and brightness was adjusted using
684 the "Min/Max" adjustment for black and white light. The pipeline from inoculation off solid plates
685 through pre-culture, growth at 39°C or 28°C, fixation, and imaging we refer to as a day's
686 experiment. We carried out 2 days' worth of experiments for each species, yielding a total of 17-
687 21 images. In each image, free-floating cells were scored manually as singlets or those with a
688 small, medium, or large bud (for a total of 31-151 scored cells per species and temperature).
689 The proportion of scored cells with large buds was tabulated for each day's experiment for each
690 species and temperature. We used these proportions (a total of two for each species and
691 temperature) as input into an ANOVA with species and temperature as factors, and took the *p*-
692 value for the interaction between the factors as the estimate of the significance of the difference
693 between species in the effect of temperature on the proportion of cells with large buds.

694

695 **Sequence analysis**

696

697 D_{xy} *analysis*.

698

699 To assess the divergence between *S. cerevisiae* and *S. paradoxus* at loci mapped by RH-seq,
700 we used the D_{xy} statistic[36], the average number of pairwise differences between all *S. cerevisiae*
701 strains and *S. paradoxus*, normalized for gene length, as follows. We downloaded *S. cerevisiae*
702 genomic sequences from the following sources: YJM978, UWOPS83-787, Y55, UWOPS05-
703 217.3, 273614N, YS9, BC187, YPS128, DBVPG6765, YJM975, L1374, DBVPG1106, K11,
704 SK1, 378604X, YJM981, UWOPS87-2421, DBVPG1373, NCYC3601, YPS606, Y12,
705 UWOPS05-227.2, and YS2 from http://www.yeastrc.org/g2p/home.do; Sigma1278b, ZTW1, T7,

706 and YJM789 from http://www.yeastgenome.org/; and RM11 from NCBI (accession
707 PRJNA13674). For each strain, we extracted the coding sequence of each gene in turn, and we
708 downloaded the *S. paradoxus* reference sequence for each orthologous coding region from [17].
709 Sequences were aligned using MAFFT[37] with default settings. Alignments that did not contain a
710 start and stop codon, or those that contained gaps at greater than 40% of sites were considered
711 poor quality and discarded. We tabulated D_{xy} for each gene. To evaluate whether the eight RH-
712 seq hit genes were enriched for elevated D_{xy}, we first tabulated $<D_{xy}>_{true}$, the mean value across
713 the eight RH-seq hit genes. We then sampled eight random genes from the set of 3416 genes
714 tested by RH-seq; to account for biases associated with lower rates of divergence among
715 essential genes, the resampled set contained six essential genes and two non-essential genes,
716 mirroring the breakdown of essentiality among the RH-seq hits. Across this random sample we
717 tabulated the mean D_{xy}, $<D_{xy}>_{resample}$. We repeated the resampling 5000 times and used as an
718 empirical *p*-value the proportion of resamples at which $<D_{xy}>_{resample} \leq <D_{xy}>_{true}$.

719

720 *Phylogenetic analysis.*

721

722 We downloaded orthologous protein coding regions for the type strains of *S. cerevisiae*, *S.*
723 *paradoxus*, and an outgroup, *S. mikatae*, from [17]. For each gene for which ortholog sequences
724 were available in all three species, we aligned the sequences with PRANK[38] utilizing the "-
725 codon" option for codon alignment. These alignments were used as input into the codeml
726 module of PAML[39], which was run assuming no molecular clock and allowing omega values to
727 vary for each branch in the phylogeny. From the resulting inferences, we tabulated the branch
728 length on the *S. cerevisiae* lineage for each gene. To evaluate whether sequence divergence of

729 the eight RH-seq hit genes showed signatures of rapid evolution along the *S. cerevisiae* lineage,
730 we used the resampling test detailed above.

731

732 **Locus effect size**

733

734 Locus effect sizes in Figure S9 were computed from the data in Figures 2B and 3 of the main
735 text as follows. For analyses in the hybrid background, for a given locus we calculated $m_{S.par}$, the
736 mean of all replicate measurements of $e_{hemizyg}/\langle e_{hybrid}\rangle$ of hemizygote strains lacking the *S.*
737 *paradoxus* allele. We took, as independent estimates of the locus effect size (each
738 corresponding to an open circle on the respective grey bar in Figure S9), each measurement of
739 $e_{hemizyg}/\langle e_{hybrid}\rangle$ of a hemizygote strain lacking the *S. cerevisiae* allele, as a ratio against $m_{S.par}$.
740 For analyses in the *S. cerevisiae* DBVPG1373 background, for a given locus we used each
741 measurement of $e_{swap}/\langle e_{parent}\rangle$ as an independent estimate of the locus effect size (each
742 corresponding to an open circle on the respective orange bar in Figure S9). For analyses in the
743 *S. paradoxus* Z1 background, for a given locus we used each measurement of $\langle e_{parent}\rangle/e_{swap}$ as
744 an independent estimate of the locus effect size (each corresponding to an open circle on the
745 respective blue bar in Figure S9).

746

747 **Data availability**

748

749 RH-seq data will be deposited in the Sequence Read Archive (SRA) upon publication.

750

751 **Code availability**

752

Custom Python and R scripts used for RH-seq data analysis are available upon request.

755 # References

756

757 1 Flint, J. & Mott, R. Finding the molecular basis of quantitative traits: successes and
758 pitfalls. *Nat Rev Genet* **2**, 437-445, doi:10.1038/35076585 (2001).
759 2 Good, B. H., McDonald, M. J., Barrick, J. E., Lenski, R. E. & Desai, M. M. The dynamics
760 of molecular evolution over 60,000 generations. *Nature*, doi:10.1038/nature24287
761 (2017).
762 3 Savolainen, O., Lascoux, M. & Merila, J. Ecological genomics of local adaptation. *Nat*
763 *Rev Genet* **14**, 807-820, doi:10.1038/nrg3522 (2013).
764 4 Allen Orr, H. The genetics of species differences. *Trends Ecol Evol* **16**, 343-350 (2001).
765 5 Nadeau, N. J. & Jiggins, C. D. A golden age for evolutionary genetics? Genomic studies
766 of adaptation in natural populations. *Trends Genet* **26**, 484-492,
767 doi:10.1016/j.tig.2010.08.004 (2010).
768 6 Wray, G. A. Genomics and the Evolution of Phenotypic Traits. *Annual Review of*
769 *Ecology, Evolution, and Systematics* **44**, 51-72 (2013).
770 7 Masly, J. P. & Presgraves, D. C. High-resolution genome-wide dissection of the two
771 rules of speciation in Drosophila. *PLoS biology* **5**, e243,
772 doi:10.1371/journal.pbio.0050243 (2007).
773 8 Greig, D. A screen for recessive speciation genes expressed in the gametes of F1 hybrid
774 yeast. *PLoS genetics* **3**, e21, doi:10.1371/journal.pgen.0030021 (2007).
775 9 Eshed, Y. & Zamir, D. An introgression line population of Lycopersicon pennellii in the
776 cultivated tomato enables the identification and fine mapping of yield-associated QTL.
777 *Genetics* **141**, 1147-1162 (1995).
778 10 Lazzarano, S. *et al.* Genetic mapping of species differences via in vitro crosses in mouse
779 embryonic stem cells. *Proc Natl Acad Sci U S A* **115**, 3680-3685,
780 doi:10.1073/pnas.1717474115 (2018).
781 11 Roop, J. I., Chang, K. C. & Brem, R. B. Polygenic evolution of a sugar specialization
782 trade-off in yeast. *Nature* **530**, 336-339, doi:10.1038/nature16938 (2016).
783 12 Steinmetz, L. M. *et al.* Dissecting the architecture of a quantitative trait locus in yeast.
784 *Nature* **416**, 326-330, doi:10.1038/416326a (2002).
785 13 Stern, D. L. Identification of loci that cause phenotypic variation in diverse species with
786 the reciprocal hemizygosity test. *Trends Genet* **30**, 547-554,
787 doi:10.1016/j.tig.2014.09.006 (2014).
788 14 Goncalves, P., Valerio, E., Correia, C., de Almeida, J. M. & Sampaio, J. P. Evidence for
789 divergent evolution of growth temperature preference in sympatric Saccharomyces
790 species. *PLoS One* **6**, e20739, doi:10.1371/journal.pone.0020739 (2011).
791 15 Salvado, Z. *et al.* Temperature adaptation markedly determines evolution within the
792 genus Saccharomyces. *Appl Environ Microbiol* **77**, 2292-2302, doi:10.1128/AEM.01861-
793 10 (2011).
794 16 Sweeney, J. Y., Kuehne, H. A. & Sniegowski, P. D. Sympatric natural Saccharomyces
795 cerevisiae and S. paradoxus populations have different thermal growth profiles. *FEMS*
796 *Yeast Res* **4**, 521-525 (2004).
797 17 Scannell, D. R. *et al.* The Awesome Power of Yeast Evolutionary Genetics: New
798 Genome Sequences and Strain Resources for the Saccharomyces sensu stricto Genus.
799 *G3 (Bethesda)* **1**, 11-25, doi:10.1534/g3.111.000273 (2011).
800 18 Hartwell, L. H. Saccharomyces cerevisiae cell cycle. *Bacteriol Rev* **38**, 164-198 (1974).
801 19 Mitra, R., Fain-Thornton, J. & Craig, N. L. piggyBac can bypass DNA synthesis during
802 cut and paste transposition. *EMBO J* **27**, 1097-1109, doi:10.1038/emboj.2008.41 (2008).

803 20 van Opijnen, T., Lazinski, D. W. & Camilli, A. Genome-Wide Fitness and Genetic
804 Interactions Determined by Tn-seq, a High-Throughput Massively Parallel Sequencing
805 Method for Microorganisms. *Curr Protoc Mol Biol* **106**, 7 16 11-24,
806 doi:10.1002/0471142727.mb0716s106 (2014).
807 21 Parts, L. *et al.* Revealing the genetic structure of a trait by sequencing a population
808 under selection. *Genome Res* **21**, 1131-1138, doi:10.1101/gr.116731.110 (2011).
809 22 Winzeler, E. A. *et al.* Functional characterization of the S. cerevisiae genome by gene
810 deletion and parallel analysis. *Science* **285**, 901-906 (1999).
811 23 Leuenberger, P. *et al.* Cell-wide analysis of protein thermal unfolding reveals
812 determinants of thermostability. *Science* **355**, doi:10.1126/science.aai7825 (2017).
813 24 Wilkening, S. *et al.* An evaluation of high-throughput approaches to QTL mapping in
814 Saccharomyces cerevisiae. *Genetics* **196**, 853-865, doi:10.1534/genetics.113.160291
815 (2014).
816 25 Neurological Disorders: Public Health Challenges. 232 (World Health Organization,
817 2006).
818 26 Sinha, H., Nicholson, B. P., Steinmetz, L. M. & McCusker, J. H. Complex genetic
819 interactions in a quantitative trait locus. *PLoS Genet* **2**, e13,
820 doi:10.1371/journal.pgen.0020013 (2006).
821 27 Guldener, U., Heck, S., Fielder, T., Beinhauer, J. & Hegemann, J. H. A new efficient
822 gene disruption cassette for repeated use in budding yeast. *Nucleic Acids Res* **24**, 2519-
823 2524 (1996).
824 28 Wetmore, K. M. *et al.* Rapid quantification of mutant fitness in diverse bacteria by
825 sequencing randomly bar-coded transposons. *MBio* **6**, e00306-00315,
826 doi:10.1128/mBio.00306-15 (2015).
827 29 Skelly, D. A. *et al.* Integrative phenomics reveals insight into the structure of phenotypic
828 diversity in budding yeast. *Genome Res* **23**, 1496-1504, doi:10.1101/gr.155762.113
829 (2013).
830 30 Langmead, B. & Salzberg, S. L. Fast gapped-read alignment with Bowtie 2. *Nat Methods*
831 **9**, 357-359, doi:10.1038/nmeth.1923 (2012).
832 31 Liti, G. *et al.* Population genomics of domestic and wild yeasts. *Nature* **458**, 337-341,
833 doi:10.1038/nature07743 (2009).
834 32 Li, H. *et al.* The Sequence Alignment/Map format and SAMtools. *Bioinformatics* **25**,
835 2078-2079, doi:10.1093/bioinformatics/btp352 (2009).
836 33 Roop, J. I. & Brem, R. B. Rare variants in hypermutable genes underlie common
837 morphology and growth traits in wild Saccharomyces paradoxus. *Genetics* **195**, 513-525,
838 doi:10.1534/genetics.113.155341 (2013).
839 34 Maurer, M. J. *et al.* Quantitative Trait Loci (QTL)-Guided Metabolic Engineering of a
840 Complex Trait. *ACS Synth Biol* **6**, 566-581, doi:10.1021/acssynbio.6b00264 (2017).
841 35 Lee, M. E., DeLoache, W. C., Cervantes, B. & Dueber, J. E. A Highly Characterized
842 Yeast Toolkit for Modular, Multipart Assembly. *ACS Synth Biol* **4**, 975-986,
843 doi:10.1021/sb500366v (2015).
844 36 Nei, M. *Molecular Evolutionary Genetics*. (Columbia University Press, 1987).
845 37 Katoh, K. & Standley, D. M. MAFFT multiple sequence alignment software version 7:
846 improvements in performance and usability. *Mol Biol Evol* **30**, 772-780,
847 doi:10.1093/molbev/mst010 (2013).
848 38 Loytynoja, A. & Goldman, N. webPRANK: a phylogeny-aware multiple sequence aligner
849 with interactive alignment browser. *BMC Bioinformatics* **11**, 579, doi:10.1186/1471-2105-
850 11-579 (2010).
851 39 Yang, Z. PAML 4: phylogenetic analysis by maximum likelihood. *Mol Biol Evol* **24**, 1586-
852 1591, doi:10.1093/molbev/msm088 (2007).

End Notes

Supplementary Information is available in the online version of the paper.

Acknowledgements The authors thank Faisal AlZaben, Anna Flury, Gina Geiselman, Justin Hong, Jake Kim, Matt Maurer, and Luke Oltrogge for technical assistance, Dave Savage for his generosity with microscopy resources, and Ben Blackman, Sam Coradetti, Avi Flamholz, Vinny Guacci, Doug Koshland, Chris Nelson, and Arjun Sasikumar for discussions. This work was supported by R01 GM120430-A1 and by Community Sequencing Project 1460 to RBB at the U.S. Department of Energy Joint Genome Institute, a DOE Office of Science User Facility. The work conducted by the latter was supported by the Office of Science of the U.S. Department of Energy under Contract No. DE-AC02-05CH11231.

Author Contributions R.B.B. and J.I.R. developed the project design; C.V.W., J.I.R., R.H. and J.C. performed experiments; C.V.W. and J.I.R. and analyzed the data; J.M.S. contributed to the development of mutagenesis and sequencing methods; A.P.A. contributed mutagenesis and sequencing reagents; I.V.G. provided technical assistance with sequencing; R.B.B. and C.V.W wrote the manuscript with input from all authors.

Author Information The authors do not declare any competing financial interests. Correspondence and request for materials should be addressed to R.B.B. (rbrem@buckinstitute.org) and J.I.R. (jeremyianroop@gmail.com).